A Detailed Look at MIMO Performance in 60 GHz WLANs

SHIVANG AGGARWAL, Institute for the Wireless Internet of Things, Northeastern University, USA
SRISAI KARTHIK NEELAMRAJU, University at Buffalo, SUNY, USA
AJIT BHAT, University at Buffalo, SUNY, USA
DIMITRIOS KOUTSONIKOLAS, Institute for the Wireless Internet of Things, Northeastern University, USA

One of the key enhancements in the upcoming 802.11ay standard for 60 GHz WLANs is the support for simultaneous transmissions of up to 8 data streams via SU- and MU-MIMO, which has the potential to enable data rates up to 100 Gbps. However, in spite of the key role MIMO is expected to play in 802.11ay, experimental evaluation of MIMO performance in 60 GHz WLANs has been limited to date, primarily due to lack of hardware supporting MIMO transmissions at millimeter wave frequencies. In this work, we fill this gap by conducting the first large-scale experimental evaluation of SU- and MU-MIMO performance in 60 GHz WLANs. Unlike previous studies, our study involves multiple environments with very different multipath characteristics. We analyze the performance in each environment, identify the factors that affect it, and compare it against the performance of SISO. Further, we seek to identify factors that can guide beam and user selection to limit the (often prohibitive in practice) overhead of exhaustive search. Finally, we propose two heuristics that perform both user and beam selection with low overhead, and show that they perform close to an Oracle solution and outperform previously proposed approaches in both static and mobile scenarios, regardless of the environment and number of users.

CCS Concepts: • **Networks** → *Network performance analysis*; *Wireless local area networks*; Network protocols.

Additional Key Words and Phrases: 60 GHz, mmWave, MIMO, IEEE 802.11ay

ACM Reference Format:
Shivang Aggarwal, Srisai Karthik Neelamraju, Ajit Bhat, and Dimitrios Koutsonikolas. 2022. A Detailed Look at MIMO Performance in 60 GHz WLANs. *Proc. ACM Meas. Anal. Comput. Syst.* 6, 2, Article 38 (June 2022), 26 pages. https://doi.org/10.1145/3530904

1 INTRODUCTION

Today, the IEEE 802.11ad WLAN standard [18] supports data rates up to 6.7 Gbps by leveraging the 14 GHz wide unlicensed spectrum centered around 60 GHz coupled with phased arrays. Although enabling multi-Gbps wireless local area communications was a significant achievement, the high throughput requirements of emerging applications, such as VR/AR, volumetric video streaming, high-bandwidth connectivity to multiple displays, video analytics, indoor and outdoor wireless backhaul, and yet unforeseen, but certain to be demanding, applications motivate exploring techniques to support even higher data rates.

A key limitation of the 802.11ad standard is that it only supports single stream transmissions, in contrast to today's 5 GHz WLANs that support simultaneous transmissions of multiple data

Authors' addresses: Shivang Aggarwal, Institute for the Wireless Internet of Things, Northeastern University, USA, aggarwal.sh@northeastern.edu; Srisai Karthik Neelamraju, University at Buffalo, SUNY, USA, neelamra@buffalo.edu; Ajit Bhat, University at Buffalo, SUNY, USA, abhat3@buffalo.edu; Dimitrios Koutsonikolas, Institute for the Wireless Internet of Things, Northeastern University, USA, d.koutsonikolas@northeastern.edu.

2476-1249/2022/6-ART38 $15.00
https://doi.org/10.1145/3530904

streams to a single client (SU-MIMO) and multiple clients (MU-MIMO). With a dramatic increase in the AP and user density in the near future, multi-user multi-stream communication in the 60 GHz band is a key factor towards scaling the capacity of future 60 GHz WLANs. To meet the demands of future applications and the ever-increasing user density, one of the key enhancements in the upcoming IEEE 802.11ay standard [19] is the support for simultaneous transmissions of up to 8 data streams via SU- and MU-MIMO that will enable future APs in the 60 GHz band to support data rates up to 100 Gbps.

However, supporting MIMO in the 60 GHz band is much more challenging than in the sub-6 GHz bands. In contrast to sub-6 GHz channels that are characterized by rich scattering, 60 GHz channels are sparse [29, 34], i.e., they are characterized by only a few dominant paths, making the separation of multiple streams at a receiver much more challenging. Hence, in addition to the user grouping policy, which affects throughput in sub-6 GHz WLANs, the throughput of MIMO transmissions in the 60 GHz band is also affected by the selected analog beams at the AP and client(s). For example, two users falling into the same transmit beam experience significant inter-user interference and cannot decode their data streams, even when zero-forcing is applied [10, 11]. Consequently, in 60 GHz MIMO WLANs, beam selection, in addition to user selection, is a critical task.

Since joint user and beam selection requires prohibitively large training and feedback overhead and is practically infeasible [10–12], decoupling the two tasks is often proposed [9, 11, 12], at the cost of suboptimal performance. However, even for a fixed user group, the overhead of trying all possible beam combinations for simultaneous transmission of m data streams is $\binom{N}{m}^2$ in the case of SU-MIMO and N^{2m} in the case of MU-MIMO, where N is the number of available analog beams in the AP's and clients' RF codebooks. While exhaustive search over all beam combinations might be acceptable for static use cases (e.g., for wireless backhaul links), it would incur prohibitively large training overhead in mobile scenarios (e.g., VR/AR), due to the constant need for beam training. As a result, a number of heuristics have been proposed in the literature, e.g., [8, 9, 11, 12, 31] to reduce this overhead.

In spite of the key role MIMO is expected to play in 802.11ay and the above-mentioned challenges associated with its practical implementation, experimental evaluation of MIMO performance in 60 GHz WLANs has been limited to date, primarily due to lack of hardware platforms that support MIMO transmissions at millimeter wave (mmWave) frequencies. Only a small number of recent works [10–12, 35] have conducted preliminary evaluations using experimental platforms based on various types of software defined radios (SDRs), e.g, WiMi [29], X60 [23], or M-Cube [35]. Since collecting channel traces with these SDRs involves significant manual labor due to their large form factor, evaluation in these works is conducted only in a single environment, typically a large open space. The performance of 60 GHz MIMO in different indoor environments, with different multipath characteristics remains largely unknown.

In this work, we fill this gap by conducting, to our best knowledge, the *first large-scale* experimental evaluation of SU- and MU-MIMO performance in indoor 60 GHz WLANs. Unlike previous studies, our study involves multiple environments with very different multipath characteristics. We analyze the performance in each environment, identify the factors that affect it, and compare it against the performance of single-stream communication (SISO). Further, we seek to identify factors that can guide beam and user selection to limit the overhead of exhaustive search and compare the performance of a large number of beam and user selection heuristics against the optimal performance obtained from exhaustive search. Our contributions and main findings are summarized as follows:

- Using an SDR-based platform that supports multi-Gbps data rates, commensurate to those supported by the 802.11ad standard, and is equipped with reconfigurable phased arrays, similar to those found in commercial-off-the-shelf (COTS) 802.11ad devices, we conduct channel measurements in multiple environments with very different multipath characteristics and collect a large channel trace dataset (250 GB). We make this dataset publicly available[1] to enable further research in single- and multi-stream communication in 60 GHz WLANs.

- We use this dataset to conduct the first large-scale experimental performance study of SU- and MU-MIMO in indoor 60 GHz WLANs via trace-driven emulation. In addition to different environments, our study considers different numbers of MIMO streams and different approaches for MIMO beam and user selection. Our study (§4) shows that, in contrast to sub-6 GHz WLANs, where almost any randomly selected user/group can achieve a high multiplexing/MIMO gain due to rich scattering [5], MIMO performance in 60 GHz WLANs strongly depends on the multipath propagation characteristics and can be very different across environments and even across locations in the same environment, while it is also affected by the user distribution and orientation. Although MIMO communication generally offers higher data rates than SISO, the gains are often suboptimal and there are cases where SISO communication is preferable. We also discuss the root causes of this highly diverse performance.
- Since the performance of MIMO depends on a number of factors, we explore whether it is possible for the AP to decide, using a simple SNR-based heuristic, if it is beneficial to enable MIMO communication for a given link or user group (§5). We find that the SISO link SNR, which is obtained via the mandatory periodic sector level sweeps in both 802.11ad and 802.11ay, can be used as a coarse-grained classifier to determine whether MIMO communication should be enabled or not. However, a more fine-grained link/user group classification (e.g., predicting the expected MIMO performance) is not possible, due to the imperfect beam patterns of practical phased arrays that result in unpredictable inter-stream interference.
- We conduct a thorough study of the overhead involved in the selection of the best MIMO beam pairs for a link or a user group (§6). Since the overhead of performing an exhaustive search over all the available beam pairs is prohibitive in real-world scenarios with mobile clients, we evaluate the performance of two types of previously proposed heuristics that rely on the angular beam separation and the SNRs from the periodic sector level sweeps, respectively. Although a heuristic using beam angular separation was shown to work well in previous works, with nodes equipped with horn antennas generating perfect conical beam patterns, we find this type of heuristics cannot be used with practical phased arrays. Similarly, we find that limiting the beam search around the best SISO beam pairs may not always result in good MIMO performance, as the best MIMO beam pairs can be very different from the best SISO beam pairs in the angular domain. We then focus on a widely used SNR-based heuristic and conduct a detailed study of how its parameters affect the tradeoff between overhead and optimal beam selection.
- We study the overhead involved in user group selection for MU-MIMO (§7). Since the overhead of exhaustively searching over all possible groups can also be prohibitive in practice, similar to the overhead of exhaustive beam searching, we propose two simple heuristics that perform both user and beam selection with low overhead, using our insights from §5 and §6, and compare their performance against other approaches from the literature. Our evaluation shows that our heuristics perform close to an Oracle solution and outperform previously proposed approaches in both static and mobile scenarios, regardless of the environment and number of users.

[1] https://bit.ly/60ghz-mimo-data

2 BACKGROUND

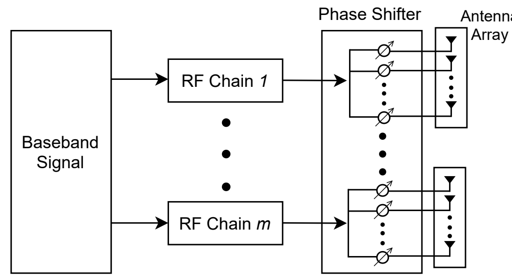

Fig. 1. MIMO Node Architecture.

We consider the node architecture in Fig. 1, which supports multi-stream communication via hybrid beamforming. A similar architecture was considered in [10, 11, 35]. The AP is equipped with multiple RF chains, one for each data stream. Client devices can be equipped with either a single RF chain (only supporting reception in MU-MIMO mode) or multiple RF chains (supporting reception in both SU- and MU-MIMO modes). While the 802.11ay standard provides support for up to 8 RF chains, we believe that hardware and power (in client devices) constraints will limit the number of RF chains in practice. Hence, we assume that nodes are equipped with at most 3 RF chains, similar to majority of legacy WiFi APs and clients.

Each RF chain is connected to a separate phased array, allowing to independently steer each stream. Following the terminology of previous works [10–12, 35], we use the terms *beam steering*, *RF beamforming*, and *analog beamforming* to refer to the selection of a directional beam (out of a predefined set of available beams) via applying different phase delays to the different antenna elements of a given phased array, and the term *beam training* to refer to the process of testing a number of beams and measuring their channels in order to select the best one. In addition, during transmission, the multiple RF chains at the AP can also be used for digital pre-coding, such as zero-forcing, at baseband to complement analog beam steering. As previous studies have shown, the performance of digital precoding depends on the choice of analog beams.

Similar to sub-6 GHz WiFi standards (802.11ac, 802.11ax), the 802.11ay standard does not specify a user selection algorithm for MU-MIMO. Recent works have proposed a number of heuristics that select a group of users either in a single-shot [9–12] or in an incremental fashion [12] leveraging SNR information obtained from periodic sector level sweeps (SLSs) between the AP and each client (which are part of both 802.11ad and 802.11ay and are used to establish and maintain the AP-client links) or knowledge of the phased array codebook (geometric shapes of the available beams).

Once a client (group of clients) is selected for a SU-MIMO (MU-MIMO) transmission, 802.11ay realizes hybrid beamforming in two stages. It first performs analog beamforming, selecting the best beam or a set of best beam candidates for each phased array, and then measures the channel with the selected beams (MIMO beam training) to implement digital beamforming. While the second stage is similar to sub-6 GHz WiFi (802.11ac/ax), the 802.11ay standard does not specify how to perform analog beamforming in the first stage, but instead proposes a number of possible options [8, 31]. Here, we consider two such options, that have also been used in other works [10–12, 35]: *exhaustive search* and *k-best*. *Exhaustive search*, which measures the channels with all possible beam combinations, can yield optimal performance, but the overhead can be prohibitive in practice. On the other hand, *k-best* ranks the beam-pairs for each AP-client pair based on SNRs obtained from the periodic SLSs and selects the top k based on SNR to test in the second stage. Clearly, *exhaustive search* is a special case of *k-best*. We also consider another special case, where $k = 1$, referred to as Single User Training (SUT) in [12], which only considers the highest-SNR beam pair for each AP-client pair, based on the periodic SLSs.

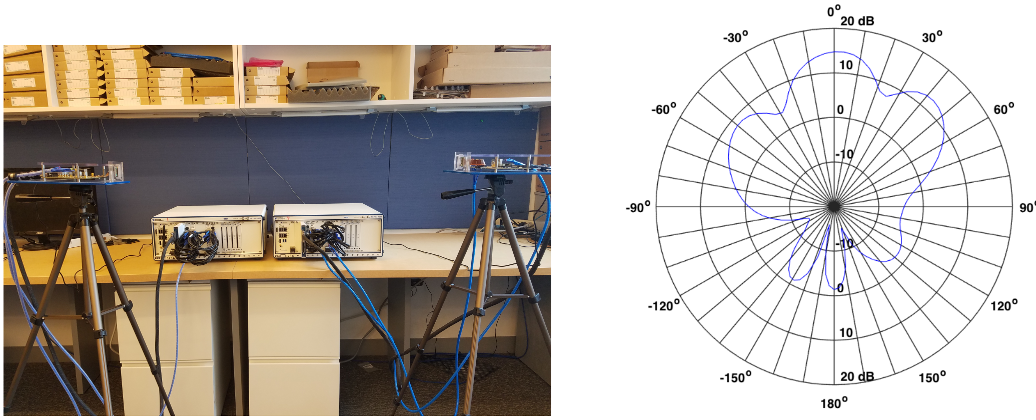

(a) Two X60 nodes. (b) Example azimuth beam pattern.

Fig. 2. X60 testbed and example beam pattern generated by X60's phased arrays.

3 SETUP AND METHODOLOGY

3.1 Experimental platform

For our experimental study, we use X60 [23] (Fig. 2a), an SDR-based 60 GHz testbed that combines fully programmable PHY and MAC layers, multi-Gbps data rates, and practical reconfigurable phased arrays. While X60 is not 802.11ad (or 802.11ay)-compliant, many of its features resemble those of 802.11ad.

Each X60 node consists of a mmWave transceiver system from NI [20] and a user-configurable phased antenna array from SiBeam. Transmissions take place over a 2 GHz wide channel, same as in 802.11ad/ay. The PHY reference implementation supports 9 Single Carrier (SC) modulation and coding schemes (MCSs) resulting in data rates from 300 Mbps to 4.75 Gbps, similar to those supported by the SC 802.11ad PHY layer. We emphasize that X60 is the *only* available programmable 60 GHz testbed that provides data rates commensurate to those supported by the 802.11ad standard. As a comparison, the reference implementation of M-Cube radio (the only available MIMO 60 GHz programmable platform) in [35], supports a channel bandwidth of only 100 MHz and a maximum data rate of only 325 Mbps.

In contrast to 802.11ad radios that use CSMA, X60 uses TDMA with 10 ms frames divided into 100 slots of 100 μs each. A slot consists of 92 codewords, each of which has an attached CRC block. For our study, which only includes scenarios involving downlink transmissions from a single AP, where CSMA is not useful, the use of TDMA instead of CSMA does not affect our conclusions. Also, note that the structure of an X60 frame resembles an 802.11 aggregated frame (AMPDU) or Transmission Opportunity (TxOP), consisting of multiple packets sent to the same user back-to-back, each with its own CRC.

The in-built phased array has 24 elements; 12 each for Tx and Rx. SiBeam's reference codebook defines 25 beam patterns that can be steered in real-time (electronic switching in $< 1\mu s$). The beams are spaced roughly 5° apart in their main lobe, thus spanning around 120° in the azimuth, from -60° to 60°. The 3 dB beamwidth ranges from 25° to 35°; hence, each beam's main lobe overlaps with several neighboring beams. The beam patterns (see Fig. 2b for an example) feature large side lobes in addition to the central main lobe, similar to the beam patterns in COTS 60 GHz devices [24, 35].

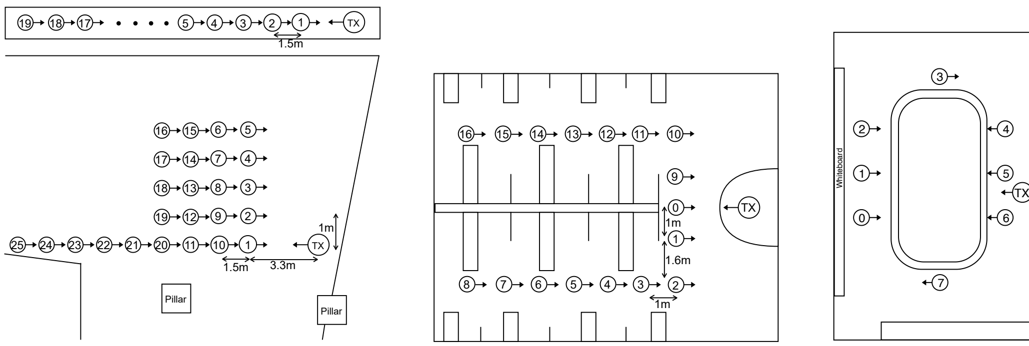

(a) Corridor (above) and Lobby (below). (b) Lab. (c) Conference Room.

Fig. 3. Measurement locations with TX/RX positions and orientations (arrows).

3.2 Experimental methodology

Since X60 does not support MIMO communication, our experimental methodology, similar to [10–12, 29], involves collecting channel samples in the time and frequency domains from over-the-air measurements between 2 X60 nodes (one acting as the AP and the other one as the client) and perform trace-driven emulation to study MIMO in 60 GHz WLANs. For each AP-client setting, we collect channel statistics for all possible 625 (25 x 25) beam-pair combinations. For each beam-pair, 100 frames are transmitted at MCS 0 and SNR, channel amplitude and phase, and power delay profile (PDP) are logged every 40 ms (every 4 frames). We assume that multiple RF chains are co-located at the AP (and at the client, in case of SU-MIMO). Previous works that used X60 for MIMO emulation [10, 11] found that changing the location of a node by $\lambda/2$ (2.5mm) does not change the received PDP, channel, and SNR, as, due to wide beamwidth of the SiBeam's codebook entries, the physical paths captured by a beam are not sensitive to small movement of the AP or client. The total size of our dataset is about 250 GB.

To emulate hybrid analog/digital beamforming for a given choice of analog beams, we process the channel traces at the AP and clients and compute zero-forcing weights. Applying the zero-forcing weights, we compute the expected SINR at each receiver and infer the per-user data rate using the X60 SNR-MCS mapping table from [1]. Then, for each user and potential multi-stream analog configuration, we select the X60 MCS index whose corresponding SNR is less than or equal to the calculated SINR. The corresponding number of data bits per symbol is the per-user data rate (according to the 802.11ay standard, each stream can use a different MCS but the coding rate for all streams is the same).

We compare the performance of SU- and MU-MIMO against the performance of SISO. In the case of a single client, the SISO throughput is obtained from the SNR-MCS mapping table using the highest SNR beam pair between the AP and the client. In the case of N clients, we obtain the data rate for each client using the same methodology. Then, we assume that the AP follows a round robin transmission schedule and calculate the aggregate SISO data rate as $R_{agg} = \sum_{i=1}^{N} R_i/N, i = 1, 2, ..., N$, where R_i is the data rate of the i-th client, if it was the only client in the network. Note that, due to the fixed frame duration (10 ms), we have time fairness rather than transmission fairness (i.e., the AP transmits for 10 ms to each client in a round robin fashion instead of sending one packet to each client). This reflects the performance of recent 802.11 standards (802.11n/ac/ad/ay) that use frame aggregation and limit the number of AMPDUs for each MCS while keeping the maximum frame aggregation time constant. Hence, the well-known rate anomaly problem [17] of older versions of 802.11 does not apply here.

3.3 Measurement locations

In contrast to previous works that collected traces in a single environment, we performed over-the-air experiments and collected channel traces in *multiple* locations within a campus building, with diverse multipath characteristics. The measurement locations, along with the TX/RX positions and orientations are shown in Fig. 3. **Lobby.** This is a large open space (Fig. 3a) with glass panels covering the upper part and metallic sheets covering the lower part of one side and a wall on the other side. There are also metallic chairs and tables scattered around. The TX and RX antennas are kept at a height of 1.4 m. **Lab.** This is an $11.8 \times 9.2 \times 3.4$ m^3 space with 4 rows of desks surrounded by metallic storage cabinets and white boards (Fig. 3b). The TX antenna is placed at a height of 2.05 m and the RX antenna at a height of 1.25 m. **Conference Room.** This is a $10.4 \times 6.8 \times 3.2$ m^3 space with a large white board covering one of the walls (Fig. 3c). There are metallic cabinets, a large desk in the center of the room, and many chairs. The TX and RX antennas are placed at a height of 1.4 m. **Corridor.** We performed measurements in a corridor (Fig. 3a) of width 1.74 m, with the TX and RX antennas at a height of 1.4 m.

Compared to the conference room, the other environments either lack the presence of many strong reflectors (lobby, corridor) or have structures that block the signal (lab), and as a result, most links could not be established at all with different orientations. Since observing performance with varying number of clients is one of the main goals of this work, we used a fixed TX-RX orientation in those environments, with the RX always facing the TX, as shown in Figs. 3a, 3b. In contrast, the conference room has multiple strong reflectors, which allowed us to conduct experiments with a more natural client orientation in that environment, as shown in Fig. 3c.

4 MIMO PERFORMANCE: CLASSIFICATION AND ANALYSIS

We begin by investigating the maximum MIMO performance possible for a given link or user group ignoring the overhead of searching for the best combination of analog beams. For each AP-client link in the case of SU-MIMO and each user group in the case of MU-MIMO, we exhaustively search over all possible combinations of beam pairs ($\binom{N}{m}^2$ for SU-MIMO, N^{2m} for MU-MIMO) and select the ones that give the maximum aggregate data rate. For SU-MIMO, we calculate the multiplexing gain for each AP-client link, defined as the ratio of the data rate achieved during MIMO communication to the data rate achieved using only a single stream to communicate. For MU-MIMO, we calculate the MIMO gain for each group, defined as the ratio of the aggregate data rate when simultaneously transmitting data to all the users in that group to the aggregate data rate achieved when transmitting data to each user separately in a round robin manner, as described in §3.2. The ideal (maximum possible) multiplexing/MIMO gain is m, where m is the number of streams used for communication. Note that, in the case of MU-MIMO, we assume that clients have a single RF chain. Figs. 4a, 4b plot the CDF of the multiplexing and MIMO gain, respectively, over all environments and links/groups in the case of 2 and 3 streams.

Figs. 4a, 4b show that, for about 80% of the links and user groups, the multiplexing/MIMO gain is more than 1, implying that *transmitting data simultaneously over multiple streams generally leads to an improvement in performance over SISO communication.* The median gain is 1.41 (1.75) in the case of SU-MIMO and 1.37 (1.94) in the case of MU-MIMO with 2 (3) streams. However, the percentage of links/groups that achieve the maximum multiplexing/MIMO gain is generally small – ~20% (~5%) of the links in the case of 2 (3) streams for SU-MIMO and only ~5% (~1%) of the groups in the case of 2 (3) streams for MU-MIMO achieve a multiplexing/MIMO gain of 2 (3). On the other hand, for about ~20% of the links/user groups, the multiplexing/MIMO gain is less than 1, regardless of the number of streams, implying that MIMO communication in those cases hurts performance.

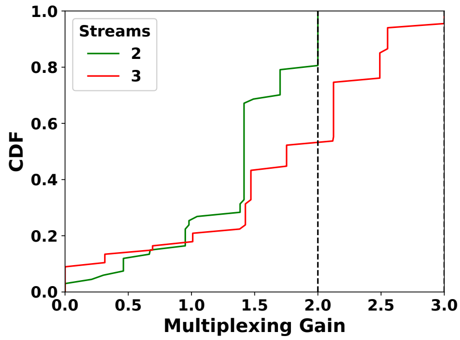

(a) SU-MIMO.

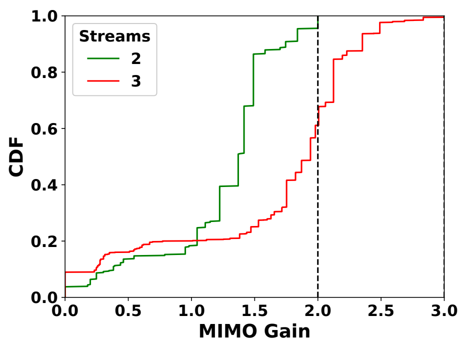

(b) MU-MIMO.

Fig. 4. Multiplexing/MIMO Gain.

Table 1. SU-MIMO User/MU-MIMO Group Categorization.

Overall	**Strong**	**Satisfactory**	**Weak**	**Total**
2 streams	21/83	29/416	18/113	68/612
3 streams	17/535	39/255	12/774	68/3864
Lobby				
2 streams	7/28	14/265	4/7	25/300
3 streams	6/275	19/2025	0/0	25/2300
Lab				
2 streams	10/45	6/75	1/0	17/120
3 streams	7/240	10/320	0/0	17/560
Conf. Room				
2 streams	1/1	2/8	4/12	7/21
3 streams	1/1	3/9	3/25	7/35
Corridor				
2 streams	3/9	7/68	9/94	19/171
3 streams	3/19	7/201	9/749	19/969

Moreover, for about ~10% (~5%) of the links/user groups in the case of 2 (3) stream communication, the multiplexing/MIMO gain is 0, i.e., MIMO communication is not possible at all.

Table 1 classifies the links in the case of SU-MIMO and user groups in the case of MU-MIMO based on their performance in 3 categories: 1) **Strong**: links/groups achieve at least 75% of the optimal multiplexing/MIMO gain, 2) **Satisfactory**: links/groups achieve multiplexing/MIMO gain of at least 1 (i.e., the MIMO performance is no worse than the corresponding SISO performance), 3) **Weak**: links/groups achieve multiplexing/MIMO gain lower than 1 (i.e., MIMO performance is worse than the corresponding SISO performance). We observe that in the Lobby and Lab environments, nearly all positions/groups result in at least satisfactory performance, i.e, MIMO performs as well as or better than SISO. In contrast, in the Conference Room and Corridor environments, for nearly half the links and up to 75% of the groups MIMO communication results in performance degradation compared to SISO communication.

One reason for the suboptimal MIMO performance for many links/groups is the fact that, during MIMO communication, the total AP's transmission power is equally split among the m streams. This results in lower Rx power at each receiver, which often leads to lower supported MCS compared to SISO communication, as shown in Figs. 5a, 5b. These figures show the MCS distribution across all environments for SU-MIMO and MU-MIMO, respectively. We observe that, as the number of streams increases, relatively lower MCS indexes are utilized. Correspondingly, the number of non-working links or groups also increases (white color in the legend) when more streams are used, as mentioned before. Nonetheless, for a large number of links/groups, the drop in MCS is not substantial and the median MIMO performance remains relatively high, albeit suboptimal, as we saw in Figs. 4a, 4b. For example, in ~50% of the cases in 3-stream communication for both SU-

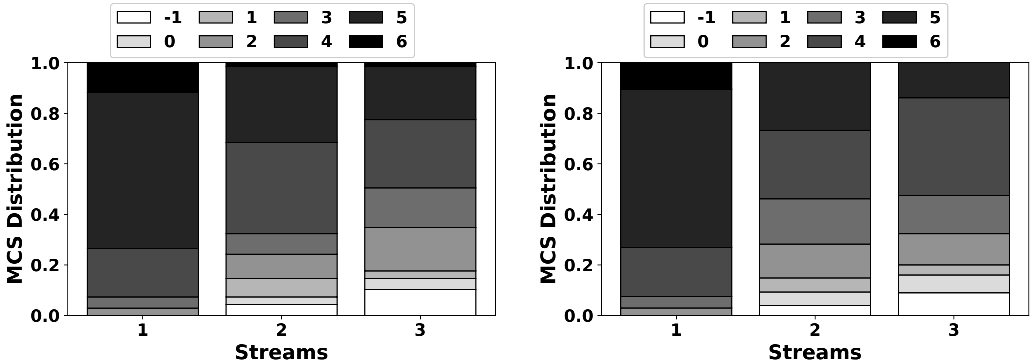

(a) SU-MIMO.

(b) MU-MIMO.

Fig. 5. Distribution of supported MCSs. We denote cases where the nodes cannot communicate at all (not even at MCS 0) as -1 in the legend (white color).

and MU-MIMO and ~65%/~50% of cases for SU-MIMO/MU-MIMO in 2-stream communication, the supported MCS is 4 or higher, corresponding to a data rate of at least 2.86 Gbps [1].

A second reason for the suboptimal MIMO performance of many links/groups is the way zero-forcing works. To cancel inter-stream interference, zero-forcing projects the channel vector of a stream on a precoding vector that is orthogonal to the channel vector of the other stream, so that the projected channels become orthogonal to each other. This comes with a penalty, which depends on the mutual correlation of the channels of different streams/users, i.e., channel projection incurs signal energy loss if the original channel vectors are not orthogonal. While in sub-6 GHz bands the rich scattering propagation causes semi-orthogonal channels and thus zero-forcing can cancel interference with low penalty, 60 GHz channels are sparse and, more importantly, the effective channel vector of each user depends on the choice of analog beams that amplifies certain paths and weakens others.

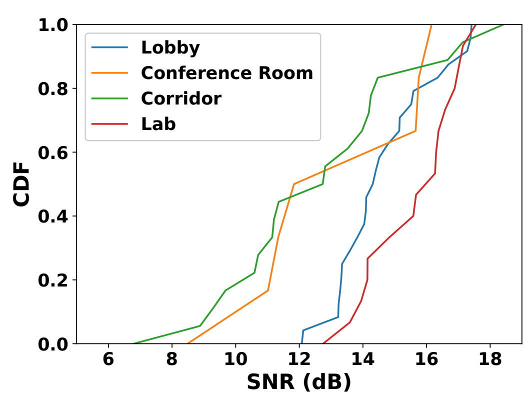

Fig. 6. CDF of SNRs obtained across all positions in each environment.

These two reasons together explain why we observe the largest number of cases where MIMO communication fails in the Corridor and the Conference Room environments (Table 1). Note that these two environments have the largest number of low-SNR links (see Fig. 6). In the Corridor, the optimal beams for SISO communication are similar for all users due to the specific user distribution (users placed in a row behind each other and all facing the AP) and the absence of strong reflectors to create alternative high-SNR beams. If those beams are used for MIMO communication, the zero-forcing penalty is high; if alternative low-SNR beams are used, they become even weaker during MIMO communication, as the transmission power is split among multiple streams, especially for users more than 15 m away from the AP. In the Conference Room, although there are several strong reflectors, some links are relatively weak due to the orientation of the user with respect to the AP (Fig. 3c): in 4 out of the 8 positions, the RX faces away from the AP, and in two other

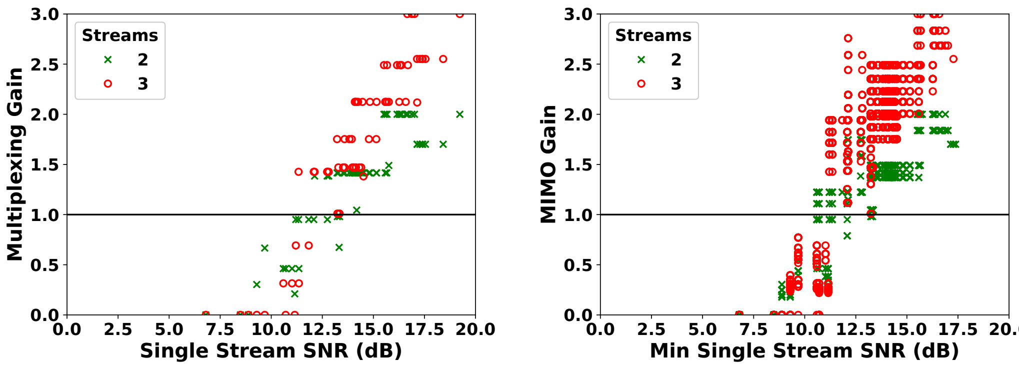

(a) SU-MIMO. (b) MU-MIMO.

Fig. 7. Single stream SNR vs. multiplexing/MIMO gain.

positions (positions 3, 7), the relative TX-RX angle is quite wide making even SISO communication challenging (recall that all 25 beams together span around 120° in the azimuth, as mentioned in §3.1). In fact, at position 7, communication was not possible even with a single stream. In contrast, in the Lobby and Lab, most links are strong, as shown in Fig. 6, and there are also several strong reflectors, resulting in good MIMO performance in most cases.

Overall, we conclude that, in contrast to sub-6 GHz WLANs, where almost any randomly selected user/group can achieve a high multiplexing/MIMO gain due to rich scattering [5], *MIMO performance in 60 GHz WLANs strongly depends on the multipath propagation characteristics, the user distribution, and the user orientation, and can be very different across environments and even across locations in the same environment.*

5 SNR-BASED MIMO PERFORMANCE PREDICTION

As we saw in the previous section, the performance improvement/degradation when using multiple streams compared to using a single stream depends on a large number of factors. In this section, we explore whether simple heuristics, based on the SNRs of the beam pairs that result in the best SISO performance, can guide the decision of whether the AP should continue using a single stream for communication or switch to communicating over multiple simultaneous data streams. Recall that the knowledge of these SNRs incurs no additional overhead, since they are obtained from the mandatory periodic SLSs. We are interested in both coarse-grained classification, i.e., simply ascertaining whether transmitting data simultaneously over multiple streams would improve performance or not, before actually enabling multi-stream communication, and in fine-grained prediction, i.e., predicting the expected multiplexing/MIMO gain of different SU-MIMO links or MU-MIMO groups.

Fig. 7a plots the SU-MIMO multiplexing gain for each link against the SNR of that link when using only a single stream for communication. We observe that, in the case of 2-stream/3-stream communication, when the single-stream SNR is less than SNR_L^{SU}=12.12 dB/11.34 dB, the multiplexing gain is always less than 1. In other words, using 2 streams/3 streams for communication always leads to a performance drop if the SNR of the beam pair that results in the best SISO performance is below SNR_L^{SU} and thus, in such cases, MIMO communication should not be used. As we observe in Fig. 6, the SNRs of several links in the Corridor and Conference Room fall below this threshold. On the other hand, if the single stream SNR is above SNR_H^{SU}=13.34 dB/11.83 dB, then the multiplexing gain with 2 streams/3 streams is always greater than 1 thus implying that we should always switch to MIMO communication in those cases. Fig. 6 shows that the SNRs of almost all links in the Lobby and all links in the Lab have SNRs above this threshold.

Similarly, Fig. 7b plots the MU-MIMO gain for each user group against the lowest SISO SNR among the users in that group. We observe that simultaneously transmitting data to 2 users/3 users always results in lower aggregate data rate compared to SISO when the single stream SNR of the weakest user in the group is less than SNR_L^{MU}=10.59 dB/11.14 dB. On the other hand, if the weakest user's SNR is greater than SNR_H^{MU}=13.32 dB/11.2 dB, multi-stream communication always leads to an improvement in aggregate data rate compared to SISO. Again, Fig, 6 shows that the SNR of several users in the Corridor and Conference Room (most users in the Lobby and Lab) fall below (above) these thresholds.

In Figs. 7a, 7b, we also observe that the MU-MIMO thresholds are slightly lower than the corresponding SU-MIMO thresholds. In the case of MU-MIMO, users are spatially separated and, in many cases, the highest SNR beam pairs are different for different users. As a result, their channels are less correlated, and hence, it is easier for zero-forcing to cancel inter-user interference. In contrast, in the case of SU-MIMO, the highest SNR beam pair for each stream is the same, as all antennas are co-located on the same node.

We conclude that *the SNR of the beam pairs that result in the best SISO performance can be used as a coarse-grained classifier*; an AP can determine whether MIMO communication for a given link/user group should be enabled or not by periodically obtaining the SISO SNRs from the SLSs and comparing them against the thresholds SNR_L^{SU}, SNR_H^{SU}, SNR_L^{MU}, SNR_H^{MU}. In practice, the AP might have to adjust these thresholds via online learning, e.g., by comparing the observed MIMO performance against the performance observed before switching to MIMO. However, a more fine-grained classification, e.g., predicting the expected multiplexing/MIMO gain, is not feasible, especially in the case of 3 streams. Figs. 7a, 7b show that, for the same SNR value, the multiplexing/MIMO gain can span a large range of values. Further, these figures show that, for a narrow range of SNRs (from 0.06 dB in the 2x2 MU-MIMO case up to 2.73 dB in the 3x3 MU-MIMO case) the multiplexing/MIMO gain can be both above or below 1, depending on the link/user group; in those cases, SNR cannot guide the decision of whether to enable MIMO communication or not.

5.1 Why is Fine-Grained SNR-Based Prediction Hard?

To understand why fine-grained MIMO performance prediction using the SISO SNRs is not feasible, we use a metric called Beam Index Difference (BID), first defined in [23]. The BID for two beam pairs, with beam indices (TX_1,RX_1) and (TX_2,RX_2), is defined as $BID = |TX_2 - TX_1| + |RX_2 - RX_1|$. Essentially, this metric shows the angular diversity amongst the two beam pairs in consideration; two beam pairs with high BID have beams whose main lobes point far from each other, and there is less chance for the corresponding channels to be highly correlated.

Fig. 8 plots the CDF of the BIDs between the best MIMO beam pairs and the beam pairs that resulted in the best SISO performance, for all links/user groups for which the SISO SNRs are higher than SNR_H^{SU}/SNR_H^{MU}. We observe that in only 3% of the cases for SU-MIMO (2- and 3-stream) and 2x2 MU-MIMO and 10% of the cases for 3x3 MU-MIMO, one of the best MIMO beam pairs is the same as the best SISO beam pair (BID=0). In the median case, the BID is 5 for both SU- as well as MU-MIMO, i.e., in 50% of the cases the best MIMO beam pairs are close to the best SISO beam pairs, but not identical. However, the 75th percentile is more than 10 (12) in the case of SU-MIMO (MU-MIMO), and the max BID is 25 (40) in the case of SU-MIMO (MU-MIMO), implying that *the best MIMO beam pairs can be very different from the best SISO beam pairs in the angular domain.* Since the beam pairs that yield optimal MIMO performance can be very different from the beam

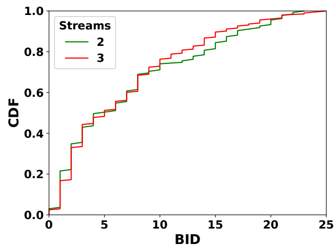

(a) SU-MIMO.

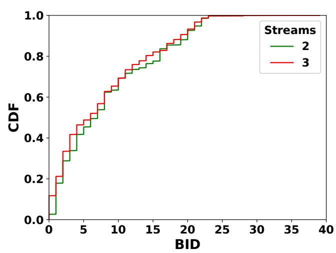

(b) MU-MIMO.

Fig. 8. BID of best MIMO beam pairs with best single stream beam pairs.

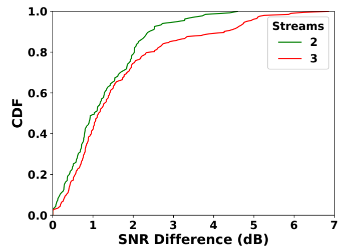

(a) SU-MIMO.

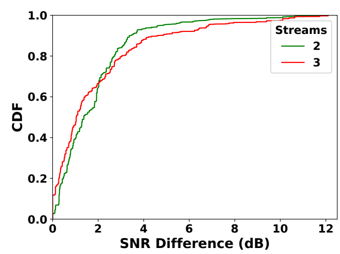

(b) MU-MIMO.

Fig. 9. SNR difference of best MIMO beam pairs with best single stream beam pairs.

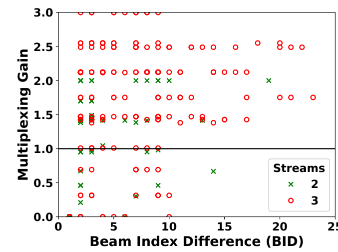

(a) SU-MIMO.

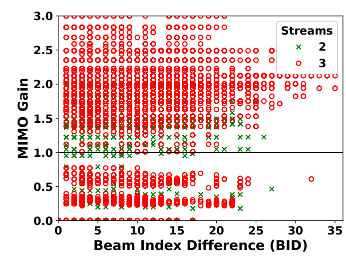

(b) MU-MIMO.

Fig. 10. BID vs. multiplexing/MIMO gain.

pairs that yield optimal SISO performance, the knowledge of the SISO SNR(s) for a (group of) user(s) cannot always predict the SU-MIMO (MU-MIMO) performance for that (group of) user(s).

To analyze why beam pairs with large BIDs from the best SISO beam pairs often result in optimal MIMO performance, we plot in Fig. 9 the CDF of the SNR difference between the best MIMO beam pairs and best SISO beam pairs. In the median case, the SNR difference is just 1 dB for both SU-MIMO and MU-MIMO and in the 80th percentile, the SNR difference is still low, 2 dB for SU-MIMO and 3 dB for MU-MIMO. This shows that *even though the beam pairs that result in optimal MIMO performance are almost always different from the best SISO beam pairs, they can still have strong SNRs* due to the strong side lobes of beam patterns generated by phased arrays and (in the case of the Lobby and Lab) the presence of strong reflectors in the environment. However, Fig. 9 also shows that the CDFs have a long tail, up to 7 dB (11 dB) in the case of SU-MIMO (MU-MIMO), i.e., in certain cases, selecting beam pairs that result in weak but orthogonal/semi-orthogonal channels is more beneficial than beam pairs that result in very strong but non-orthogonal channels. Since the highest link SNR in our measurement environments is 16-18 dB (Fig. 6), this further suggests that the beam pairs that yield optimal MIMO communication can have SNRs significantly lower than the lower thresholds (SNR_L^{SU}, SNR_L^{MU}) defined based on Fig. 7 (10-12 dB) based on the SNRs of the SISO beam pairs, and explains again why a fine-grained classification based only on the SNRs of the SISO beam pairs is not possible.

6 MIMO BEAM SELECTION OVERHEAD

Until now, we have looked at the highest multiplexing/MIMO gain that can be achieved for a given link/user group using the optimal set of beam pairs and ignoring the overhead of searching for that optimal set. However, depending on the number of beams in the AP's and client's codebooks, the overhead to search over all possible combinations of beam pairs can be prohibitively large. In our X60 testbed, each node can transmit/receive data using 25 different beams (§3.1). Using the same IEEE 802.11ay parameters as in [10], the time required to perform an exhaustive search over all possible combinations of beam pairs for 3x3 MIMO communication is about 484 ms (more than 4x longer than the typical 802.11 beacon interval of 100 ms) for SU-MIMO and over 22 s for MU-MIMO. In typical AP-client scenarios with mobile clients, where search has to be performed frequently, these overheads are prohibitively large. In the rest of this section, we study various heuristics for reducing the beam selection overhead. We consider two approaches: BID-based and SNR-based.

6.1 BID-Based Heuristics

The work in [12], proposed a heuristic that selects beam pairs based on the BID metric and showed that it achieves satisfactory performance in the case of small groups (consisting of 2 or 3 users, similar to the cases we consider in this work). The rationale is that selecting beam pairs with large angular separation should result in reduced inter-stream interference, and hence, strong MIMO performance. However, the authors in [12] performed their evaluation with horn antennas that generate perfect conical beams, resulting in lower inter-stream interference. To explore why such a heuristic would work in practical settings with nodes equipped with phased arrays, we plot in Fig. 10 the multiplexing/MIMO gain for each link/user group against the BID between the beam pairs resulting in optimal performance when using multi-stream communication.[2] We observe that there is no correlation between BID and the multiplexing/MIMO gain; the same BID can result in multiplexing/MIMO gain anywhere between 0 and m. The reason is that practical phased arrays generate imperfect beams with strong sidelobes, as explained in §5.1, and hence, it is not straightforward to predict the amount of inter-stream interference based on the angular separation of the main lobes alone.

Another simple heuristic to potentially reduce this overhead is, instead of performing an exhaustive search, to search only a small subset of beam pairs around the best SISO beam pairs, assuming that the channels of such beam pairs should be strong enough to reduce inter-stream interference. Our analysis in §5.1, Fig. 8 shows that such a heuristic would select the optimal beam pairs for MIMO communication only about 50% of the time.

6.2 SNR-Based Heuristics

***k-best* heuristic.** Another approach to limit the number of beam pairs to search, and thus reduce the MIMO beam training overhead, is the *k-best* heuristic, which is included in 802.11ay and has also been explored in other works, as we explained in §2. To explore the effectiveness of this heuristic, we rank the beam pairs resulting in optimal MIMO performance across all links/user groups and environments on the basis of their SISO SNRs (e.g., if a beam pair used in a MIMO link/user group has rank 1, this means that the same beam pair has the highest SNRs among all beam pairs and is the one that is used for SISO communication for that link/user). Fig. 11 plots the CDF of the ranks in the case of 2 and 3 streams. We observe that, in the median case, for both SU- and MU-MIMO, the beam pairs that result in the best 2-stream/3-stream MIMO performance are among the top 10 beam pairs in terms of their SNRs during SISO communication. However, we also observe that there is a large tail in the CDFs for both SU- and MU-MIMO.

[2] If we try to extend the BID definition in the case of 3x3 MIMO as $BID = |TX_2 - TX_1| + |RX_2 - RX_1| + |TX_3 - TX_1| + |RX_3 - RX_1| + |TX_3 - TX_2| + |RX_3 - RX_2|$, there is no direct correlation between the metric and the angular separation, as there are multiple beam pair combinations with very different angular separation but the same BID, e.g., beam pairs (1,1), (13,13), (25,25) and (1,1), (1,1), (25,25) both have BID=96, but the second combination clearly has poor angular separation overall, with two beam pairs being identical, which is detrimental to MIMO performance, since the channels will not be orthogonal. Instead, we only define BID for the case of two beam pairs, and in the case of 3x3 MIMO in Fig. 10, we include 3 different BIDs for each 3x3 MIMO link/user group, calculated as $BID_1 = |TX_2 - TX_1| + |RX_2 - RX_1|$, $BID_2 = |TX_3 - TX_1| + |RX_3 - RX_1|$, $BID_3 = |TX_3 - TX_2| + |RX_3 - RX_2|$.

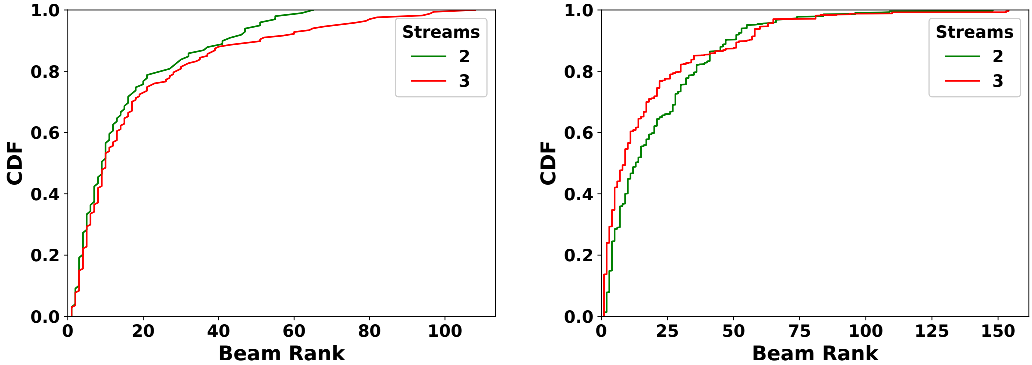

(a) SU-MIMO.

(b) MU-MIMO.

Fig. 11. Ranks of best MIMO beam pairs amongst best single stream beam pairs.

For SU-MIMO, overall, the best MIMO beam pairs are among the top 60/top 100 SISO beam pairs for 2-stream/3-stream MIMO communication. Hence, if we limit the search for the best MIMO beam pairs for 3-stream communication to the top 100 beam pairs instead of searching exhaustively over all 625 available beam pairs for each stream, this would result in a significant drop in the MIMO beam searching overhead from 484.36 ms to just 1.72 ms, thus *making SU-MIMO beam searching much more practical while at the same time achieving near-optimal performance.*

In the case of MU-MIMO, we observe that, in some cases, the best performing MIMO beam pairs may not even be in the top 100 SISO beam pairs. Further, even if we were to search only among the top 100 beam pairs, this would still incur an overhead of 91.88 ms (almost one typical beacon interval), which may not be ideal in practical, mobile scenarios. Thus, *in the case of MU-MIMO, there is a need to limit the search even further in terms of beam selection and balance the tradeoff between the performance and the beam training overhead.*

Overhead analysis for MU-MIMO. Due to the dynamic channel conditions in practical scenarios with mobile clients, the optimal set of beam pairs might change over time. Thus, MIMO beam training needs to be performed periodically to react quickly to these changes. The selected *beam training period* is another important parameter that will affect the above mentioned tradeoff. To evaluate this tradeoff, we perform again trace-driven emulations with *k-best* for different *beam training periods* and *k* values. We consider 5 different *k* values – 1 (SUT), 10, 20, 50, 100 – and we vary the *beam training period* from as low as 10 ms to as high as 500 s. For all possible user groups in all user environments, and for each value of *k* and *beam training period*, we calculate the aggregate MU-MIMO PHY data rate by taking into account the time consumed to perform the MIMO beam training, which is performed once every *beam training period.*[3] Note that depending on the *k* value, the resulting MIMO performance may not be optimal as the the optimal set of beam pairs may be excluded from the search. However, the lower the *k*, the lower will be the overhead of performing the beam search, thus leading to higher channel utilization albeit at a potentially lower data rate. Figs. 12, 13 plot, for 2-stream MU-MIMO and for 3-stream MU-MIMO, respectively, the 25th, 50th, and 75th percentile of the aggregate PHY data rates across all links/user groups over all environments for each *k* and *beam training period.* For comparison, we also show in Table 2 the

[3]Note that the MIMO beam training overhead is in addition to the overhead of the periodic SLSs (SISO beam training). Since these SLSs are mandatory in both 802.11ad and 802.11ay, we do not consider their overhead in our emulation.

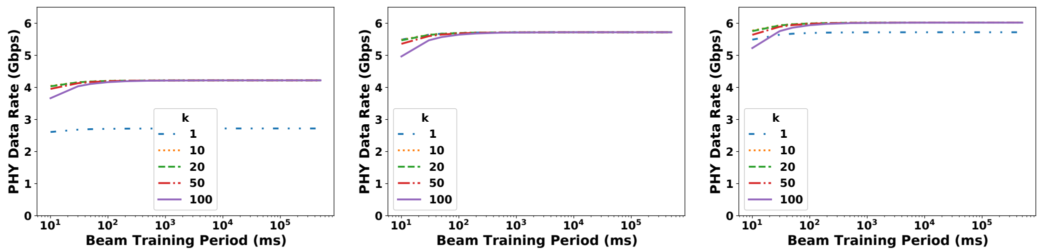

(a) 25th percentile. (b) 50th percentile. (c) 75th percentile.

Fig. 12. Data rate achieved by varying the k and *beam training period* for 2-stream MU-MIMO.

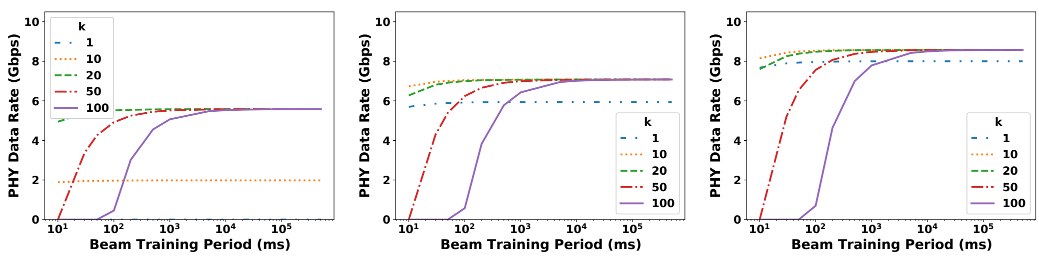

(a) 25th percentile. (b) 50th percentile. (c) 75th percentile.

Fig. 13. Data rate achieved by varying the k and *beam training period* for 3-stream MU-MIMO.

MIMO data rate with k=625 (exhaustive search) ignoring the MIMO beam searching overhead, i.e., assuming an oracle that always selects the best beam pairs for MIMO communication.

Table 2. Oracle MU-MIMO data rate in Gbps (25th, 50th, and 75th percentiles).

	25th	50th	75th
2-stream	4.22	5.72	6.02
3-stream	5.58	7.08	8.58

In the case of 2-stream MU-MIMO, at the 25th percentile (Fig. 12a), with k=1, there is a loss of >1 Gbps in terms of data rate compared to the other values of k irrespective of the *beam training period*. For all other values of k, the loss in data rate is minimal and actually, for *beam training periods* longer than 100 ms, the difference between their performance and the performance of the Oracle (Table 2) is negligible. The same holds true in the median case (Fig. 12b) and the 75th percentile (Fig. 12c) as well, for all values of k including k=1. This shows that *for 2-stream MU-MIMO, even with a small k value of just 10, we are able to find near optimal beam pairs and even for the shortest beam training period of 10 ms, the resulting data rate is close to the optimal due to the lower beam training overhead with the small k.*

For 3-stream MU-MIMO, at the 25th percentile (Fig. 13a), we observe that, if we just use the best SISO beams for MIMO communication (k=1), MU-MIMO communication cannot be established at all, while even for k=10, the drop in performance compared to the performance obtained with higher values of k can be >3 Gbps. On the other hand, with higher k values of 50 and 100, the performance remains low for *beam training periods* in the 100s of ms (more than 1 s with k=100) but is the same as the Oracle's for longer *beam training periods*. The reason is that with higher k, the beam training overhead is high, and thus when the *beam training period* is low, the channel utilization is low as well. We observe a similar trend for k 50 and 100 in the 50th (Fig. 13b) and 75th (Fig. 13c) percentiles. The performance with k=1 is much closer to the performance achieved with higher k values in the 50th and 75th percentiles and k=10 has the highest performance among all the k values for these percentiles. Overall though, across the 25th, 50th and 75th percentiles, we can

Algorithm 1 *SNR-B*

```
function GetMIMOGroup(PrimaryUser)
    g = {PrimaryUser}
    UserSet = {User_1, User_2, .., User_n} − PrimaryUser
    for i = 1 to m − 1 do
        User = arg min_{User_j} |SNR_SISO(User_j) − SNR_SISO(PrimaryUser)|, User_j ∈ UserSet
        if SNR_SISO(User) > SNR_H^MU then
            g = g + User
            UserSet = UserSet − User
    return g
for each TxOP do
    PrimaryUser = UPDATE_PRIMARY_USER()
    if SNR_SISO(PrimaryUser) > SNR_H^MU then
        MU group g = GetMIMOGroup(PrimaryUser)
        Select beam pairs for g using k-best approach
        Transmit data to g (MIMO) using selected beam pairs
    else
        Transmit data to PrimaryUser alone (SISO) using highest SNR_SISO beam pair
```

see that *k=20 finds beam pairs that result in near optimal performance while keeping the beam search overhead low, about 1.13 ms per beam training period. Thus, with this k, we can select a relatively low beam training period (30 ms results in minimal loss in performance) to quickly react to any sudden changes in channel conditions due to user mobility, blockage, or interference.*

Since our analysis for both SU-MIMO and MU-MIMO in this section is based on the 802.11ay parameters, we expect our recommendations for the values of k and *beam training periods* to be valid for any 802.11ay-compliant radios with phased arrays similar to those used in X60. For example, the authors in [35] obtained good performance for 2x2 SU-MIMO with M-Cube nodes equipped with phased arrays from COTS radios using k=50, which is agrees with our results in Fig. 11a.

7 MULTI-USER MIMO GROUP SELECTION

In the previous section, we looked at the beam selection overhead for MIMO communication. For SU-MIMO, once the decision is made to use MIMO for a particular user, the beam selection overhead is the only overhead that needs to be incurred. However, for MU-MIMO, another important task, that needs to be performed before analog beam selection, is user grouping, i.e., deciding which users to include in the MU group such that there is a benefit in performing MIMO communication over SISO communication. In this section, we propose and evaluate new group selection heuristics and compare their performance to existing heuristics from the literature. For each heuristic, we assume that the AP always has data available for all users and it serves users in a round-robin fashion; it serves each user for a single TxOP, and then moves on to serve the next user.

7.1 Heuristics

Based on our findings from §5, we propose two simple heuristics for group selection, to guarantee an improvement in performance when performing MU-MIMO over SISO communication: *SNR-B* (SNR-Based, Algorithm 1) and *RSNR-B* (Random SNR-Based, Algorithm 2). We describe these heuristics assuming 1 AP equipped with m RF chains and n users, each equipped with 1 RF chain.

Algorithm 2 *RSNR-B*

```
PossibleMIMOGroups = Set of all possible MIMO groups
CheckedMIMOGroups = ∅
function GetMIMOGroup(PrimaryUser)
    g = {PrimaryUser}
    UserSet = {User_1, User_2, .., User_n} − PrimaryUser
    for i = 1 to m − 1 do
        User = arg min_{User_j} |SNR_SISO(User_j) − SNR_SISO(PrimaryUser)|, User_j ∈ UserSet
        if SNR_SISO(User) > SNR_H^MU then
            g = g + User
            UserSet = UserSet − User
    return g
function GetMIMOGroupRandom(PrimaryUser)
    g = {PrimaryUser}
    UserSet = {User_1, User_2, .., User_n} − PrimaryUser
    while Size(g) < m or Size(UserSet) > 0 do
        User = random(UserSet)
        if SNR_SISO(User) > SNR_H^MU then
            g = g + User
        UserSet = UserSet − User
    return g
for each TxOP do
    PrimaryUser = update_primary_user()
    if SNR_SISO(PrimaryUser) > SNR_H^MU then
        if First round of TxOPs in progress then
            MU group g = GetMIMOGroup(PrimaryUser)
            Select beam pairs for g using k-best approach
        else if CheckedMIMOGroups != PossibleMIMOGroups then
            g_random = {PrimaryUser}
            do
                MU group g_random = GetMIMOGroupRandom(PrimaryUser)
                if g_random == {PrimaryUser} then
                    break
            while g_random in CheckedMIMOGroups
            if g_random != {PrimaryUser} then
                CheckedMIMOGroups = CheckedMIMOGroups + g_random
                Select beam pairs for g_random using k-best approach
                if Throughput(g_random) > Throughput(g) then
                    g = g_random
        Transmit data to g (MIMO) using selected beam pairs
    else
        Transmit data to PrimaryUser alone (SISO) using highest SNR_SISO beam pair
```

SNR-B. In each TxOP, the AP first decides whether it should try to form a MU group between the primary user and other users or just perform SISO communication, using the SNR threshold values for SNR_H^{MU} defined in §5. If the SISO SNR for that user is above the threshold, then the AP finds up to $m-1$ other users that have the closest SISO SNRs to the primary user's SISO SNR considering only those users with SISO SNRs higher than SNR_H^{MU}. Then, it performs beam selection for the selected MU group using the *k-best* approach with a k value of 20 (§6). If the SISO SNR of the selected user is lower than SNR_H^{MU}, or if there are no other users with SISO SNR higher than SNR_H^{MU}, the AP does not form a MU group and serves that user alone (SISO communication) using the beam pair with the highest SISO SNR.

RSNR-B. The second heuristic has an incremental change on top of *SNR-B*. Once the AP has completed its first round of TxOPs by serving all the users at least once and the groups are formed based on the logic described for *SNR-B*, in each corresponding round, *RSNR-B* forms a new group with the primary user in each TxOP by adding up to $m-1$ random users with SISO SNRs higher than SNR_H^{MU}, and performs MIMO beam training using *k-best*. If this new group results in higher performance (estimated using the computed zero-forcing weights after MIMO beam training), then *RSNR-B* uses the new group in the current TxOP, otherwise it reverts back to the previously chosen group. *RSNR-B* repeats this process for each subsequent round, testing a new random group in each round among those groups that have not been tested yet for that primary user, until it has tried each possible group. At that point, *RSNR-B* would have found the optimal group for that primary user and continues using the optimal group for the remaining data packets. Similar to *SNR-B*, *RSNR-B* uses k=20. The rationale behind this heuristic is the finding in §5 that SISO SNR cannot be used for fine-grained user group classification. Since the same SNR value can result in very diverse MIMO gains for different user groups, it makes sense to test all eligible groups. The price one pays with *RSNR-B* is the higher overhead compared to *SNR-B*, as *RSNR-B* incurs the overhead of MIMO beam selection in each round (in addition to every *beam training period*) until all groups have been tested. In contrast, *SNR-B* performs MIMO beam selection only in each *beam training period*, since it always uses the same group. However, if the selected group has suboptimal performance, *SNR-B* never has a chance to discover the best group.

We compare the performance of these two heuristics with 2 heuristics proposed in [10]: *Interference-aware Incremental Partitioned Multi-test (I^2-PM)* and *Exhaustive Decoupled*.

I^2-PM. *I^2-PM* starts by partitioning all the users into m partitions based on their SISO SNRs, where m is the number of streams supported by the AP. It sorts the users based on their SISO SNRs in descending order and then puts the $\lceil U/m \rceil$ users with the highest SNRs in the first partition, followed by the next set of $\lceil U/m \rceil$ highest SNR users in the second partition, etc., where U is the total number of users. Then, for the primary user, it tries to form a user group in an incremental fashion. In the first round, it finds the partition the primary user belongs to (say partition i) and tests all the users in the following partition ($i+1 \pmod m$) by calculating the MIMO performance when grouped with the primary user. This process continues in the following $m-2$ rounds, testing all users in partitions ($i+2 \pmod m$) in the 2nd round, ($i+3 \pmod m$) in the 3rd round, etc., until either a group of m users is formed or adding new users to the group does not improve the aggregate MIMO performance. The *I^2-PM* heuristic utilizes the SUT mechanism (k=1) for beam selection.

Exhaustive Decoupled. The *Exhaustive Decoupled* heuristic tests all possible user groups of up to m users with the pre-selected user in that round to find the MU group that results in the highest MIMO performance utilizing, similar to *I^2-PM*, the SUT approach for beam selection. This heuristic will naturally result in extremely high overhead for group selection, especially with a large number of users.

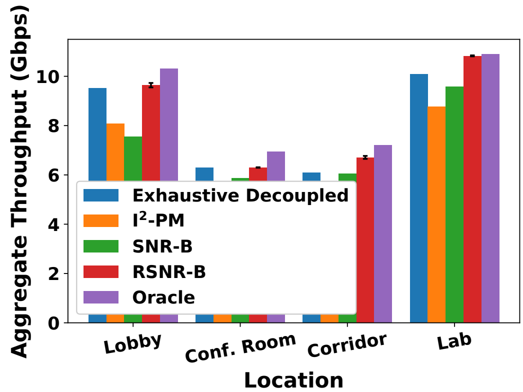

Fig. 14. Performance of group selection heuristics assuming zero group/beam selection overhead.

In [12], *I^2-PM* was shown to perform very close to *Exhaustive Decoupled* when the overhead is ignored and to outperform all heuristics proposed in that work, including *Exhaustive Decoupled*, when the overhead is taken into account.

We also compare the performance with an *Oracle* solution that instantly knows the best set of users to form an MU group with each primary user and the set of beam pairs for that group that result in the optimal performance.

Note that all four heuristics considered in this section are standard compliant and can be easily implemented on COTS 802.11ay devices, as they only rely on the SISO SNRs obtained from the mandatory periodic SLSs.

7.2 Methodology

We run trace-based emulations in all 4 environments where we collected traces assuming a single AP with 3 RF chains and multiple clients, each with a single RF chain. In each round, depending on the heuristic, we attempt to form a group with the primary user (the user whose turn is to be served in the current TxOP) and other users, and then perform beam training for the selected group based on the appropriate beam training parameters: k, which varies depending on the heuristic and the *beam training period*, which we select as 30 ms for all heuristics for fairness based on our findings in §6. We set the TxOP duration to 10 ms.

7.3 Zero Overhead Performance Comparison

We begin by comparing the performance of the heuristics assuming zero overhead for both group selection and beam searching. Fig. 14 plots the aggregate MIMO throughput for each of the heuristics in all four environments in our dataset. In each case, we run a 10 second emulation and we assume there are users present at all locations for which we collected traces. We make the following observations.

First, the absolute throughput values in the Lobby and Lab are much higher than those in the Corridor and Conference Room. This follows our finding in §4, where we saw that, in the Lobby and Lab, nearly all MU-MIMO groups result in MIMO gain more than 1, while in the Corridor and Conference Room, more than half the groups resulted in performance degradation, and hence, there are many cases where the heuristics decide to perform SISO communication.

Second, irrespective of the environment, the *RSNR-B* approach performs nearly optimally (>90% of *Oracle*), while *SNR-B* achieves between 75% and 90% of *Oracle*'s performance. This shows that, in general, our group selection heuristics pick strong MU groups resulting in high MIMO performance.

RSNR-B performs better than *SNR-B* in all environments, since it tries a different group in each round and is able to discover better groups at zero overhead (recall that we ignore the overhead in this section). In contrast, *SNR-B* often selects suboptimal groups, especially in the Lobby, where there are many users with strong SNRs.

Third, the *Exhaustive Decoupled* heuristic achieves ~90% of *Oracle*, as it exhaustively searches over all groups to find the best one but uses the SUT mechanism for beam selection, leading to this ~10% performance drop from the *Oracle* (note that in Fig. 11b the best MIMO beam pairs have rank 1 only in 15% of the 2-stream cases and 1% of the 3-stream cases).

Fourth, interestingly, we observe that I^2*-PM* manages to achieve ~80% of the *Oracle*'s performance in the environments with mostly strong users (Lobby, Lab), however, in environments with a more diverse set of users in terms of SNR (Conference Room, Corridor), it is able to achieve only ~50% of the *Oracle*'s performance. The root cause of this lies in the way I^2*-PM* partitions its users. Due to I^2*-PM*'s partitioning technique, the last (in our case 3rd, as m=3) partition ends up having all the weak users in the Corridor and Conference Room (see Table 1). Consequently, this heuristic can never form a 3-user group in these two environments, which hurts overall performance with respect to the other heuristics. Note that, in [12], I^2*-PM* was shown to perform within 84% of the *Oracle* in an open space environment, similar to the Lobby in this work, when the overhead is ignored. Our evaluation in diverse environments show that the performance of this heuristic highly depends on the environment.

7.4 Impact of Overhead

We now evaluate the performance of the different heuristics by taking into account the group selection as well as beam selection overhead in our emulation. Note that here we still assume that the *Oracle* incurs zero overhead to find the best group and beam selection. In addition, in this section, we vary the number of users present in each environment as opposed to always considering users at each location where we collected traces. We vary the user set size in multiples of 5 up to the maximum users in each environment. For each user set size, we run the emulation 100 times and each time we randomly select the corresponding number of users out of all the available locations. Fig. 15 plots, for all environments, the average and standard deviation of the aggregate MIMO throughput achieved across all the emulations for each heuristic and user set size. We make the following observations.

First, irrespective of the environment, the performance of *Exhaustive Decoupled* drops significantly as the number of users increases. For example, in the Lobby, for 5 users, it achieves ~80% of the *Oracle*'s performance, but when the number of users increases to 25, its performance drops down to just ~7%. This is expected as, when the number of users increases, the overhead to exhaustively search through all possible user groups increases substantially as well, thus hurting channel utilization.

Second, the I^2*-PM* heuristic, similar to what we observed in §7.3, performs significantly worse in the Conference Room (Fig. 15b) and Corridor (Fig. 15c) than in the Lobby (Fig. 15a) and Lab (Fig. 15d), achieving just ~50% of the *Oracle*'s performance in the first two environments vs. ~75% in the last two. As we noted in §7.3, this is due to the difference in the diversity of users in terms of their SNRs amongst the 2 sets of environments.

Third, across environments, the performance of the I^2*-PM* heuristic generally improves and becomes more stable (lower standard deviations) with higher number of users. This is due to the fact that with more users in total, there are more users in each partition, thus giving the heuristic more options to find a better performing MU group. Note that, in [12], I^2*-PM* was evaluated only with 40 users and the standard deviations were found to be negligible, which agrees with our results

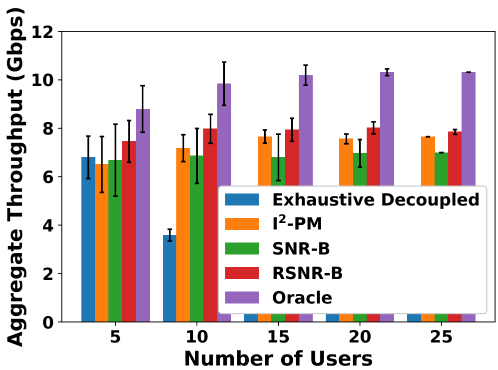

(a) Lobby.

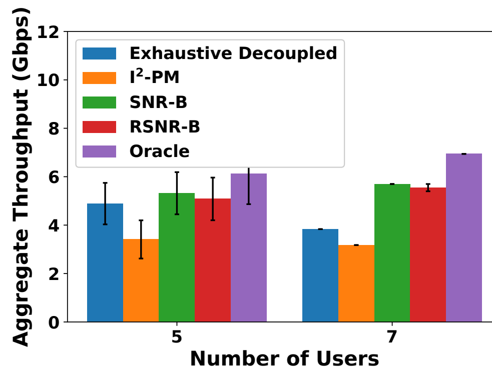

(b) Conference Room.

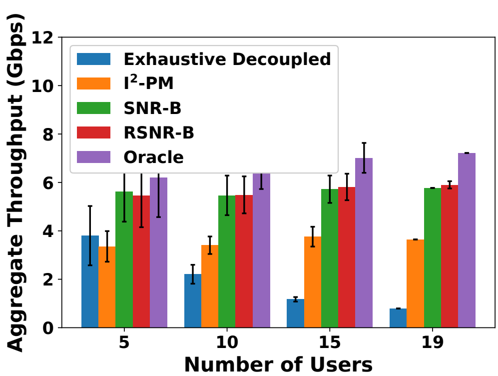

(c) Corridor.

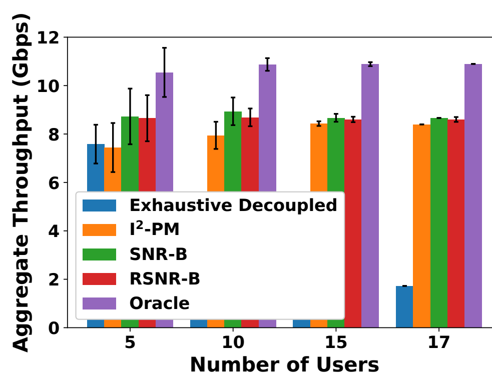

(d) Lab.

Fig. 15. Performance of group selection heuristics including the impact of overhead for different sets of users.

for large number of users. However, for small numbers of users (e.g., 5), our results show that the performance of *I^2-PM* can vary a lot in all four environments depending on the user positions.

Fourth, irrespective of environments and number of users, *SNR-B* and *RSNR-B* achieve the highest MIMO aggregate performance among all the heuristics, achieving ~80% of the *Oracle*'s performance (the only exception is for *SNR-B* in the Lobby, where its performance is slightly lower at ~70% of *Oracle*'s performance). This shows that *SNR-B*'s and *RSNR-B*'s group selection algorithms, in addition to working well in all locations (as we have seen in §7.3), also pick high performing MU groups for all user set sizes while keeping the beam selection overhead reasonably low.

In addition to performing slightly worse than *RSNR-B* (and even than *I^2-PM* in the Lobby), *SNR-B* also exhibits higher standard deviations, especially for small numbers of users, as in those cases, there is a higher probability for it to select a suboptimal group. In contrast, *RSNR-B* tries a different group in each round and, when the number of users is small, it is able to test all the groups and select the optimal group for each primary user, which leads to better performance in spite of the higher overhead.

Table 3 shows the channel utilization for each heuristic in each environment with the maximum number of users in that environment, calculated as the percentage of time spent transmitting data out of the total time (data plus overhead). Expectedly, *Exhaustive Decoupled* has the lowest channel utilization ranging from as low as 7.7% in the Lobby (25 users) to 60.8% in the Conference Room (7

Table 3. Channel utilization (%) comparison for the maximum number of users in each environment.

	Lobby	Conf. Room	Corridor	Lab
SNR-B	92.5	96.9	95.4	90.4
RSNR-B	83	88.3	87.5	82.3
I^2-PM	94.7	98.2	97.5	95.6
Exhaustive Decoupled	7.7	60.8	12.7	17.2

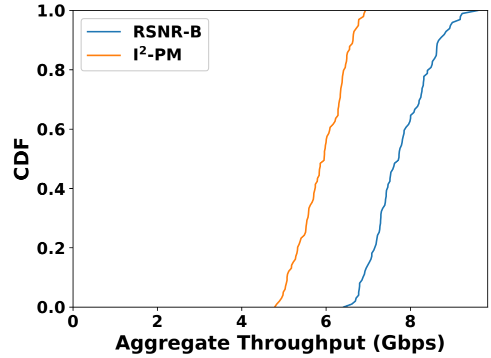

Fig. 16. Performance of *RSNR-B* and *I^2-PM* heuristics under mobility.

users). On the other hand, *I^2-PM* has the highest channel utilization among all the heuristics, as it does not incur MIMO beam selection overhead and, compared to *Exhaustive Decoupled*, it only searches 1/3 of the users in each round and completes the search in the first 2 rounds, incurring zero user selection overhead afterwards. However, its suboptimal beam selection (SUT) and partitioning technique hurts its performance, as we explained before. *SNR-B* has slightly lower channel utilization than *I^2-PM* but still offers better performance due to the higher k utilized for beam selection and its better group selection. We also see that, for *RSNR-B*, the channel utilization is even lower (82%-88%) compared to *SNR-B*, as it performs beam training for a new group in each round until it exhausts all possible groups. However, *RSNR-B* still results in better performance than *I^2-PM* and has either comparable or better performance than *SNR-B* in all cases, because it is able to discover and use better user groups that offset the higher overhead of finding those groups.

Overall, we conclude that, SNR-B *and* RSNR-B *perform consistently well irrespective of the environment and the number of users, and* RSNR-B *offers more stable and either comparable or better performance than* SNR-B *in spite of its higher overhead.* On the other hand, *I^2-PM* fails to perform well in environments where there is a mix of strong and weak users, or when the number of users is small, as its low overhead (lowest among all heuristics) is offset by its poor beam selection and partitioning algorithm.

7.5 Mobility

Finally, we evaluate the performance of *I^2-PM* and *RSNR-B* under a mobility scenario. We pick the Lobby environment and consider the grid of positions 1-20 (Fig. 3a). We repeat the emulation 100 times, each with 5 users. In each emulation, we randomly select a set of 5 positions among the 20 possible positions, which we assume are the starting positions of the 5 users. Then, once every second, each user decides whether to stay at their current position (50% probability) or to move to a new position. If a user decides to move, the user uniformly randomly chooses a direction (left, right, up, or down) and moves to the adjacent position in that direction. This emulates a scenario where users are gathered in a large, open space, with some of them occasionally moving (e.g., to chat with nearby users). In addition to the MIMO beam training interval of 30 ms, we assume a SISO beam training interval of 100 ms, which is the typical SISO beam training interval in 60 GHz COTS devices.

Note here that there might be cases when the users have moved but neither the SISO beam training interval nor the MIMO beam training interval has elapsed. In such cases, all heuristics will continue using the previously chosen groups and beam pairs, which might result in suboptimal performance. Also, at the beginning of each MIMO beam training period, the MIMO beam selection may be performed with stale SISO SNRs (those obtained in the last SISO beam training period), which may also lead to suboptimal performance. In this case, if any user in the group supports only MCS 0, it is removed from the group, and if MIMO communication fails completely, we switch to SISO communication until the next SISO beam training period (group thrashing [28]).

Fig. 16 plots the CDF of the aggregate MIMO throughput across all the 100 emulations for both *I^2-PM* and *RSNR-B*. In the median case, *RSNR-B* achieves an aggregate throughput of 7.71 Gbps while *I^2-PM* achieves 5.9 Gbps. We observe that this gap in performance between the 2 heuristics is quite consistent across all percentiles. We conclude that, even *under mobility,* RSNR-B *results in notably better performance, accomplishing a 30% improvement in aggregate throughput over I^2-PM.*

8 DISCUSSION AND FUTURE WORK

In this section, we discuss a few aspects of the MIMO performance that we did not consider in this study, a few limitations of our study, and some possible extensions of our work.

Impact of beamwidth. In addition to the number of beams, the beamwidth is another factor that affects the beam training overhead and the MIMO performance. Intuitively, wider beams can significantly reduce the beam search time at the cost of lower antenna gain (and hence, lower throughput), while narrower beams can steer the energy better towards the receiver to achieve higher throughput, at the cost of higher beam training overhead. The SiBeam phased arrays used in X60, similar to the phased arrays of most COTS 802.11ad devices (e.g., ASUS ROG Phone, ASUS ROG Phone II, Netgear Nighthawk X10 router, TP-Link Talon AD7200 router, Airfide router, Acer TravelMate P648 laptop) do not allow us to vary the beamwidth, and hence, we did not study its impact in this work. Nonetheless, we note that the impact of beamwidth and its associated tradeoff between throughput and beam training time is already well known (e.g., the works in [12, 13] have already studied it extensively in the context of 60 GHz MIMO WLANs using radios equipped with horn antennas).

Impact of blockage/mobility. Since this is the first large-scale study of MIMO performance in 60 GHz WLANs, we focused on other factors that affect performance, primarily in static scenarios, and we only briefly considered mobility in a single scenario in §7.5. Similarly, the works in [10, 35] briefly studied the impact of blockage in a few simple scenarios. An extensive study of the impact of mobility and blockage and the combined effect of both factors on MIMO performance in 60 GHz WLANs is part of our future work.

Emulation vs. real-world experiments. As we mentioned in §3.1, X60 is the only available programmable 60 GHz testbed that provides data rates commensurate to those supported by the 802.11ad standard, however, it does not support MIMO communication. Consequently, our study is based on emulation using traces collected from over-the-air experiments. In contrast, M-Cube [35], the only available programmable 60 GHz MIMO platform, supports a channel bandwidth of only 100 MHz and a maximum data rate of only 325 Mbps. Since we wanted to study the impact of MIMO on performance in 802.11ay 60 GHz WLANs, we opted to trade-off some fidelity in the PHY layer (which is unavoidable in emulation) for observing true Gigabit/s performance (as expected in 802.11ay), which is only possible with a platform like X60 that supports a bandwidth of 2 GHz. Comparing the results we obtained from trace-based emulation over a wideband channel vs. those obtained from real measurements over a narrowband channel (using M-Cube) is an interesting avenue for future work.

Extension to 5G mmWave radios. In addition to future 802.11ay-compliant 60 GHz WLANs, MIMO is also part of the 5G NR standard. 5G mmWave, being primarily an outdoor wireless technology, has very different link characteristics compared to 802.11ay, which is an indoor WLAN standard, operates in different (lower) frequency bands (28 GHz and 39 GHz), and relies on a different architecture. We believe that some of the heuristics we studied in this work for reducing the beam and user group selection overhead might also be applicable to 5G mmWave. However, a detailed study of MIMO performance in outdoor settings using 5G NR radios is necessary to draw accurate conclusions.

9 RELATED WORK

9.1 MIMO in sub-6 GHz WLANs

A large number of works has studied the problem of user selection in sub-6 GHz WLANs, e.g., [4, 5, 7, 21, 28, 30, 33], either leveraging channel state information [7, 21, 28, 30] or exploiting the rich scattering propagation in indoor environments below 6 GHz [4, 5, 33]. Some works focus on theoretical results [7, 30] while others [4, 21, 28, 33] provide practical implementations and evaluations using SDRs or COTS radios. Our work studies MIMO performance in the 60 GHz mmWave band, which lacks the rich scattering properties of the sub-6 GHz bands, making the problem of user selection more challenging. Further, each RF chain is connected to a phased array, and hence analog beamforming is also required in addition to digital beamforming. The only work that studies hybrid beamforming in sub-6 GHz WLANs is [6]. The authors consider a node architecture similar to the one we consider in this work, and propose decoupled beam-user selection strategies based on the power and Angle-Of-Arrival of the LOS path for every user. However, this works assumes a multi-carrier system and assigns different carriers to each user to reduce the training overhead. In contrast, we focus on single-carrier 802.11ad/ay WLANs.

9.2 MIMO in mmWave Networks

Theoretical work. Several works have studied hybrid beamforming in mmWave networks, focusing on developing theoretical low-complexity algorithms that can achieve near-optimal capacity performance [2, 3, 16, 25, 27]. These works do not address user selection. The work in [9] proposes a simple heuristic for user selection using SNRs in 802.11ad WLANs and evaluates it using simulations. A few recent works [14, 15, 22] provide theoretical results on joint beam-user selection in multi-cell cellular outdoor mmWave networks, while our focus is on single-cell indoor WLANs.
Experimental Work. Experimental work on mmWave MIMO is limited, primarily due to lack of hardware platforms that support MIMO transmissions at mmWave frequencies, as we mentioned in §1. The works in [26, 32] demonstrate experimentally the benefits of beamforming and spatial multiplexing in outdoor environments, considering static and vehicular scenarios, respectively. The work in [26] conducts measurements at 28 GHz and 73 GHz, using traces collected with horn antennas, which generate perfect conical beam patterns, while the work in [32] uses ray-tracing simulations. In contrast, we focus on indoor WLANs and conduct over-the-air measurements using practical phased arrays, similar to those found in COTS 802.11ad radios, which generate imperfect beam patterns with strong sidelobes.

The works in [10–12, 29, 35] are the ones closest to our work, as they focus on MIMO communication in 60 GHz indoor WLANs. The authors in [29] were the first to report measurement-based results for a 2x2 60 GHz SU-MIMO link using an SDR equipped with horn antennas. Their main finding was that co-located antennas may experience similar Friis loss pattern, thus impairing the MIMO potential, especially at short distances. The authors in [10, 11] propose a practical beam selection algorithm for MIMO 60 GHz WLANs and evaluate it using X60 but they do not consider user selection. The authors in [12] use traces collected with X60 to demonstrate that the selection of beams and users are tied to each other but decoupling the two results in a small capacity loss when there are many users in the network. They then propose and evaluate a number of disjoint beam and user selection strategies, including *Exhaustive Decoupled* and I^2*-PM*, which we also include in our study, using measurements with horn antennas. These works conduct all the measurements in an open space. In contrast, we conduct the first large-scale evaluation of MIMO in 60 GHz WLANs, considering different indoor environments with very different propagation characteristics. As we saw in §7, the performance of I^2-*PM* can be very different in different environments. Note that all these works adopt the same methodology as ours, i.e., they perform trace-driven emulation using traces collected with a SISO SDR.

The authors in [35] built M-Cube, the first experimental 60 GHz MIMO platform, by combining an SDR and phased arrays from COTS 802.11ad radios, and conducted limited experiments in indoor and outdoor environments. They found that the *k-best* strategy with k=50 yields good results in the case of 2x2 SU-MIMO (which agrees with our findings), but k=1 yields good results in the case of 2x2 MU-MIMO (which contradicts our findings as well as those in [10, 11]). Unlike X60, which supports a 2 GHz channel bandwidth and provides Gbps data rates commensurate to those in COTS 802.11ad radios, the SDR used in M-Cube only supports a 100 MHz channel bandwidth and data rates up to a few 100s of Mbps. In addition, our study is much more extensive considering 3x3 MIMO in addition to 2x2, user selection in addition to beam selection, and a variety of environments.

10 CONCLUSION

In this paper, we conducted the first large-scale experimental evaluation of SU- and MU-MIMO performance in 60 GHz WLANs using a large channel trace dataset collected in a variety of environments. We analyzed the performance in each environment, identified the factors that affect it, and compared it against the performance of SISO. In addition, we explored the feasibility of using SNR to perform an informed decision of whether MIMO communication should be enabled for a given link/user group or not and performed a detailed study of the overhead-performance tradeoff involved in beam and user selection. Finally, we proposed two heuristics that perform both user group and beam selection with low overhead and showed that they perform close to an Oracle solution and outperform previously proposed approaches in both static and mobile scenarios, regardless of the environment and number of users.

ACKNOWLEDGMENTS

We thank our shepherd, Prof. Jia Liu, and the anonymous reviewers for their valuable comments. This work was supported in part by the National Science Foundation grants CNS-2139930 and CNS-2128476.

REFERENCES

[1] Shivang Aggarwal, Urjit Satish Sardesai, Viral Sinha, and Dimitrios Koutsonikolas. 2020. An Experimental Study of Rate and Beam Adaptation in 60 GHz WLANs. In *Proc. of ACM MSWiM*.

[2] Ahmed Alkhateeb, Omar El Ayach, Geert Leus, and Robert W Heath. 2014. Channel Estimation and Hybrid Precoding for Millimeter Wave Cellular Systems. *IEEE Journal of Selected Topics in Signal Processing* 8, 5 (2014), 831–846.

[3] Ahmed Alkhateeb, Geert Leus, and Jr. Robert W. Heath. 2015. Limited feedback hybrid precoding for multi-user millimeter wave systems. *IEEE Trans. on Wireless Comms.* 14, 11 (2015), 6481–6494.

[4] Narendra Anand, Jeongkeun Lee, Sung-Ju Lee, and Edward W. Knightly. 2015. Mode and user selection for multi-user MIMO WLANs without CSI. In *Proc. of IEEE INFOCOM*.

[5] Ehsan Aryafar, Narendra Anand, Theodoros Salonidis, and Edward Knightly. 2010. Design and Experimental Evaluation of Multi-User Beamforming in Wireless LANs. In *Proc. of ACm MobiCom*.

[6] Zhe Chen, Xu Zhang, Sulei Wang, Yuedong Xu, Jie Xiong, and Xin Wang. 2017. BUSH: Empowering large-scale MU-MIMO in WLANs with hybrid beamforming. In *Proc. of IEEE INFOCOM*.

[7] Mounir Esslaoui, Felip Riera-Palou, and Guillem Femenia. 2012. A fair MU-MIMO scheme for IEEE 802.11ac. In *Proc. of IEEE ISWCS*.

[8] Felix Felhauer, Dana Ciochina, Thomas Handte, Nabil Loghin, and Fares Zenaidi. 2016. Low Complexity Beamtraining for Hybrid MIMO. *IEEE802.11-16/0316r0* (2016).

[9] Jian Geng, Zaixue Wei, Nanxi Li, Chao Chen, and Dacheng Yang. 2013. An efficient multi-user scheme for the 60 GHz wireless system with low cost arrays. In *Proc. of IEEE VTC Spring*.

[10] Yasaman Ghasempour, Muhammad Kumail Haider, Carlos Cordeiro, and Edward W. Knightly. 2019. Multi-User Multi-Stream mmWave WLANs with Efficient Path Discovery and Beam Steering. *IEEE JSAC* 37, 12 (2019), 2744–2758.

[11] Yasaman Ghasempour, Muhammad Kumail Haider, Carlos Cordeiro, Dimitrios Koutsonikolas, and Edward Knightly. 2018. Multi-Stream Beam-Training for mmWave MIMO Networks. In *Proc. of ACM MobiCom*.

[12] Yasaman Ghasempour, Muhammad Kumail Haider, and Edward W. Knightly. 2018. Decoupling Beam Steering and User Selection for MU-MIMO 60 GHz WLANs. *IEEE/ACM ToN* 26, 5 (2018), 2390–2403.

[13] Yasaman Ghasempour and Edward Knightly. 2017. Decoupling Beam Steering and User Selection for Scaling Multi-User 60 GHz WLANs. In *Proc. of ACM MobiHoc*.

[14] Yasaman Ghasempour, Narayan Prasad, Mohammad Khojastepour, and Sampath Rangarajan. 2017. Link packing in mmWave networks. In *Proc. of IEEE ICC*.

[15] Yasaman Ghasempour, Narayan Prasad, Mohammad Khojastepour, and Sampath Rangarajan. 2017. Managing analog beams in mmWave networks. In *Proc. of IEEE Asilomar*.

[16] Yasaman Ghasempour, Narayan Prasad, Mohammad Khojastepour, and Sampath Rangarajan. 2019. Novel combinatorial results on downlink MU-MIMO scheduling with applications. In *Proc. of IFIP WONS*.

[17] Martin Heusse, Franck Rousseau, Gilles Berger-Sabbatel, and Andrzej Duda. 2003. Performance Anomaly of 802.11b. In *Proc. of IEEE INFOCOM*.

[18] IEEE 802.11 Working Group. 2012. IEEE 802.11ad, Amendment 3: Enhancements for Very High Throughput in the 60 GHz Band. (2012).

[19] IEEE 802.11 Working Group. 2017. Enhanced throughput for operation in license-exempt bands above 45 GHz. *IEEE P802.11ay/D0.3* (2017).

[20] National Instruments. 2017. Introduction to the NI mmWave Transceiver System Hardware - National Instruments. http://www.ni.com/white-paper/53095/en/

[21] Raja Karmakar, Samiran Chattopadhyay, and Sandip Chakraborty. 2019. Intelligent MU-MIMO User Selection With Dynamic Link Adaptation in IEEE 802.11ax. *IEEE Trans. on Wireless Comms.* 18, 2 (2019), 1155–1165.

[22] Antonios Michaloliakos, W.C. Ao, and Konstantinos Psounis. 2016. Joint user-beam selection for hybrid beamforming in asynchronously coordinated multi-cell networks. In *Proc. of IEEE ITA*.

[23] Swetank Kumar Saha, Yasaman Ghasempour, Muhammad Kumail Haider, Tariq Siddiqui, Paulo De Melo, Neerad Somanchi, Luke Zakrajsek, Arjun Singh, Roshan Shyamsunder, Owen Torres, Daniel Uvaydov, Josep Miquel Jornet, Edward Knightly, Dimitrios Koutsonikolas, Dimitris Pados, Zhi Sun, and Ngwe Thawdar. 2019. X60: A Programmable Testbed for Wideband 60 GHz WLANs with Phased Arrays. *Computer Communications* (2019).

[24] Daniel Steinmetzer, Daniel Wegemer, Matthias Schulz, Joerg Widmer, and Matthias Hollick. 2017. Compressive Millimeter-Wave Sector Selection in Off-the-Shelf IEEE 802.11 ad Devices. In *Proc. of the 11th ACM CoNEXT*.

[25] R. A. Stirling-Gallacher and Md. Saifur Rahman. 2015. Multi-user MIMO strategies for a millimeter wave communication system using hybrid beamforming. In *Proc. of IEEE ICC*.

[26] Shu Sun, Theodore S. Rappaport, Jr. Robert W. Heath, Andrew Nix, and Sundeep Rangan. 2014. MIMO for millimeter-wave wireless communications: Beamforming, spatial multiplexing, or both? *IEEE Communications Magazine* 52, 12 (2014), 110–121.

[27] Xuyao Sun, Chenhao Qi, and Geoffrey Ye Li. 2019. Beam training and allocation for multiuser millimeter wave massive MIMO systems. *IEEE Trans. on Wireless Comms.* 18, 2 (2019), 1041–1053.

[28] Sanjib Sur, Ioannis Pefkianakis, Xinyu Zhang, and Kyu-Han Kim. 2016. Practical MU-MIMO user selection on 802.11ac commodity networks. In *Proc. of ACM MobiCom*.

[29] Sanjib Sur, Vignesh Venkateswaran, Xinyu Zhang, and Parmesh Ramanathan. 2015. 60 GHz Indoor Networking Through Flexible Beams: A Link-Level Profiling. In *Proc. of ACM SIGMETRICS*.

[30] Tomoya Tandai, Hiroki Mori, and Masahiro Takagi. 2009. Cross-layer-optimized user grouping strategy in downlink multiuser MIMO systems. In *Proc. of IEEE VTC Spring*.

[31] Alireza Tarighat, Payam Torab, Brima Ibrahim, Vipin Aggarwal, and Vinko Erceg. 2015. A Framework for MIMO Operation over mmWave Links. *IEEE802.11-15/0334r0* (2015).

[32] Song Wang, Jingqi Huang, and Xinyu Zhang. 2020. Demystifying Millimeter-Wave V2X: Towards Robust and Efficient Directional Connectivity Under High Mobility. In *Proc. of ACM MobiCom*.

[33] Xiufeng Xie and Xinyu Zhang. 2014. Scalable user selection for MU-MIMO networks. In *Proc. of IEEE INFOCOM*.

[34] Hao Xu, Vikas Kukshya, and Theodore S. Rappaport. 2002. Spatial and temporal characteristics of 60-GHz indoor channels. *IEEE JSAC* 20, 3 (2002), 620–630.

[35] Renjie Zhao, Timothy Woodford, Teng Wei, Kun Qian, and Xinyu Zhang. 2020. M-Cube: A Millimeter-Wave Massive MIMO Software Radio. In *Proc. of ACM MobiCom*.

Received February 2022; revised March 2022; accepted April 2022